Ab Initio Calculations on Low-Energy Conformers of α-Cyclodextrin

Cleber P. A. Anconi,[†] Clebio S. Nascimento, Jr.,[†] Juliana Fedoce-Lopes,[†] Hélio F. Dos Santos,[‡] and Wagner B. De Almeida*,[†]

LQC-MM, Laboratório de Química Computacional e Modelagem Molecular, Departamento de Química, ICEx, Universidade Federal de Minas Gerais (UFMG), Campus Universitário, Pampulha, Belo Horizonte, MG, 31270-901, Brazil, and NEQC, Núcleo de Estudos em Química Computacional, Departamento de Química, ICE, Universidade Federal de Juiz de Fora (UFJF), Campus Universitário, Martelos, Juiz de Fora, MG, 36036-330, Brazil

Received: August 3, 2007; In Final Form: September 23, 2007

In this article we carried out a comprehensive investigation of true minima on the potential energy surface (PES) for the α-cyclodextrin molecule using ab initio Hartree−Fock (HF) and density functional theory (DFT) quantum chemical methods, employing basis sets ranging from 6-31G(d,p) to 6-311++G(2d,2p) triple-ζ quality. Thermodynamic quantities and the solvent effect were evaluated at the DFT level of theory. We believe that the most relevant conformers present on the multidimensional PES were sampled in our work, using an adequate treatment of electron correlation effects to describe the intramolecular hydrogen bonds that are present in cyclodextrin species. We present new structures not reported so far and discuss, in detail, the relevance of the DFT gas-phase equilibrium structures for the experimental and theoretical studies involving cyclodextrins and corresponding inclusion complexes, in the condensed phase. In addition, among the various true minimum energy structures located on the DFT PES, the preferred structures in the gas phase and aqueous media, needed to be used as representative minima on the PES in further studies involving the interaction of α-cyclodextrin with other species, were unambiguously identified.

Introduction

Cyclodextrin (CD) is a cyclic oligomer of α-D-glucose structured by the action of certain enzymes on starch. Generally described as shallow truncated cones, cyclodextrins present a hydrophobic cavity of different sizes, depending on the number of elementary glucose units, and two different rims, a wider (head) containing all secondary hydroxyl groups and a narrower (tail) containing all primary hydroxyl groups. There are three cyclodextrins readily available having six, seven, or eight glucose units named α-CD, *β*-CD, and *γ*-CD, respectively. The applicability of cyclodextrins is closely related to the ability of this class of carbohydrate to form inclusion complexes with a very wide range of guest species in aqueous solutions.[1,2] The importance and use of CDs in the supramolecular context have been widely addressed in the literature. Due to its unique architecture, these molecules can be employed in synthesis of a large number of molecular devices such as molecular reactors, molecular nanotubes, molecular wires, and molecular shuttles.[3−6] In addition, CDs have been also used in molecular recognition due to their stereoseletivity.[7−10]

The inclusion complexation comprises secondary interactions often of solvophobic nature. In general, each weak interaction such as van der Waals, hydrophobic, or hydrogen-bonding is not sufficient individually to lead to inclusion complex formation. Thus, the driving force responsible for the inclusion phenomena is the sum of such interactions.[11] Furthermore, it cannot be ignored that those interactions may be strongly affected by the geometry of the species involved in complexation. In addition, a remarkable aspect, the nonrigidity of CDs, plays an important role in inclusion complex formation.[12]

Therefore, the structural elucidation of CDs and their complexes, in solid and in solution, is fundamental to understand host−guest interaction. In this respect, theoretical information, associated with classical characterization techniques, can play an expressive role to clarify fundamental aspects concerning the chemistry of CD complex formation, being useful for experimentalist interpretation. Nonetheless, the size of the CDs and their compounds make theoretical investigation a difficult task. Due to the existence of a complex potential energy surface (PES) for this class of compounds, more than one structure should be taken into account in theoretical studies, fundamentally the most populated species at ambient temperature.[13,14] The choice of the theoretical methodology is important to correctly interpret and compare results. Despite distinct levels of theory available, the computational cost usually plays a decisive role in the choice; therefore, care is necessary. Classical mechanics-based theoretical methodologies can be applied to systems containing a considerable number of atoms, due to low computational effort demanded in such calculations. The approximate form of force fields and their small degree of flexibility provide strongly dependable structures which could show poor geometries. Therefore, due to the poor description of interaction energies, theoretical investigation based on classical mechanics, such as molecular mechanics (MM), even when performed with a considerable number of conformers, should not give reliable information.[15] Another classical method in current use, molecular dynamics (MD), has been frequently applied in studies concerning CD complexes.[16−20] Nonetheless, the results obtained can be sensitive to the length of the dynamic simulation.[21] On the other hand, the choice of one quantum

* To whom correspondence should be addressed. Fax: 55 31 3-499-5700. E-mail: wagner@netuno.qui.ufmg.br.
[†] Universidade Federal de Minas Gerais.
[‡] Universidade Federal de Juiz de Fora.

10.1021/jp0762424 CCC: $37.00
Published on Web 11/13/2007

mechanical method is strongly dependent on the number of atoms present in the systems to be modeled and the use of such methodology may be criticized, if the solvent effects, which are known to play an important role in the complex formation, are neglected.[15]

The large size of the CD's precludes the use of computational methods based on high-level ab initio molecular orbital theory. In spite of that, considerable experience has been acquired combining distinct theoretical methodologies, such as semiempirical and density functional theory (DFT), to obtain reliable structures and interaction energies of hydrated CD's systems.[22,23] Very recently, an alternative and efficient procedure was proposed to make feasible quantum mechanical calculations of CD's aggregates, in particular of hydrated species.[24] It was pointed out that through the use of a mixed basis set, the computational costs can be considerably reduced, allowing the inclusion of electronic correlation effects in the calculations and increasing the quality of the theoretical results, by employing DFT-based methods.[24]

If we keep in mind the complexity of the multidimensional PES for isolated CDs, at least representative low-energy minimum structures should be considered in quantum mechanical investigations. In the gas phase, on the basis of chemical sense, the most representative structures are those which favor the largest number of hydrogen bonds. Recently, gas-phase structures of free CDs that contain a complete hydrogen bond belt in the wider size and all possible alcohol−alcohol type hydrogen bonds in the narrower size have been discussed.[25] There is no doubt about the stability of such kind of spatial arrangement in the gas phase, despite the almost closed cavity displayed in the conformers reported. However, depending on the size of the guest molecule, one cannot obtain an inclusion complex using such primary hydroxyl spatial disposition. Besides, these hydroxyl groups could be forbidden to make hydrogen bonds with solvent molecules.

The main experimental structures resolved for α-cyclodextrin reported hydration water molecules in their crystal data.[26−28] These works attested that water molecules located inside the cavity were capable of maintaining the conformational state of cyclodextrins in solid state, as has been extensively discussed in crystallographic studies.[26−29] According to the available literature, the exclusion of the solvent molecules from inside the cavity can occur before or simultaneously with the inclusion of the guest molecule. In the same way, their exclusion could govern a conformational change necessary to accommodate the guest molecule providing a complete understanding of the mechanism of complex formation which produces inclusion compounds.[10b,11,30,31] In this context, a more complete study of the minimum energy conformations of free α-cyclodextrin, mainly in solution, can produce important data for understanding the inclusion mechanism of guest molecules.

In this article, we carried out a quantum mechanical study concerning α-CD and pursued the structures which contain the maximum possible number of hydrogen bonds as well as other conformers sampled in the ab initio PES. We performed ab initio Hartree−Fock (HF) and DFT calculations to study the relative energies for what we believe to be the most representative α-CD conformers employing our previously reported methodology,[24] allowing the use of 6-31G(d,p) and 6-311++G(2d,2p) triple-ζ quality basis sets, to all structures investigated. In addition, harmonic frequencies that are needed to evaluate thermodynamic quantities (along with geometrical parameters) were calculated with the fully optimized DFT geometries and also the solvent effect was assessed using the polarized continuum model (PCM) to clarify our fundamental discussion about the stability of these structures including the aqueous medium effect. On the basis of our previous works[22−24,31] and in the theoretical results presented here, we discuss the existence of such structures in the gas phase and in condensed state and the relevance to further studies involving cyclodextrin inclusion compounds.

Theoretical Details

Cyclodextrins can form different types of intramolecular hydrogen bonds from the interaction of primary and secondary hydroxyl groups with either OH groups or glycosidic oxygens of adjacent glucoses. In this sense, to investigate the relevant stationary points on the PES of α-cyclodextrin, six distinct conformations chosen with criterion among various other minima were fully optimized without any geometrical or symmetry constraints using HF and DFT levels of theory. These conformations were selected to assess the main possibilities of intramolecular hydrogen-bond formation. The procedure used for finding stationary points on the PES of α-CD consists basically of a comprehensive search using a low computational semiempirical level of theory,[22,23] followed by a single point energy calculation at the HF or DFT level, and then the best candidate structures are selected on the basis of ab initio relative energies. Various DFT functionals, such as BLYP,[32,33,34] were employed in the calculations. What concerns the HF and BLYP geometry optimizations and single point calculations is they have been done using mixed basis sets as described in ref 24, where a better quality basis set was attributed to all oxygen and some selected hydrogen atoms to describe O···H interactions more appropriately and consequently the hydrogen bonds. In this approach, the STO-3G[35,36] minimum basis set was assigned to the remaining CH_n groups. The mixed basis sets, named here MBS, were defined as for MBS1 6-31G(d,p)[37] for O−H and STO-3G for CH_n and for MBS2 6-311++G(2d,2p)[38] for O−H and STO-3G for CH_n. It was shown in ref 24 that the use of mixed basis set (MBS1) for the calculation of relative energies for α-CD hydrated monomer, dimer, trimer, and tetramer leads to an average deviation with respect to the full 6-31G(d,p) basis set calculation of 6% (systematically underestimating the relative energies), which adds confidence to the use of MBS where cyclodextrins are concerned. In addition, HF and BLYP harmonic frequency calculations were carried out at the BLYP/MBS1 level of theory for all structures, characterizing them as true minima on the PES (all frequencies are real). The harmonic frequencies and fully optimized geometrical parameters were then used for the evaluation of the thermodynamic quantities, such as entropy, with the aid of the well-known formulas of statistical thermodynamics.[39]

The crystallographic data used in our studies for comparison were obtained from the Cambridge Crystallographic Data Center[40] (CCDC). These structures provide distinct geometries for the α-CD in the solid state. The structure named here X-ray I was obtained by the deposition code CHXAMH[26,27] and shows a hexahydrated structure with two water molecules located inside the cavity almost coincident with the α-CD molecular axis and four water molecules surrounding it, stabilized by hydrogen bonds between them. The other crystal structure, named X-ray II, which was deposited with the GOQZUH41 code at the CCDC data bank,[40] has no water molecules included in the cavity; however, there are four hydration molecules outside the α-CD cavity defining a hydrogen-bond chain. The hydration water molecules were not considered in the search for stationary points on the BLYP/MBS1 PES for the free α-CD species.

To evaluate the plausibility of existence of the obtained gas phase α-CD conformers in the condensed phase, the solvent

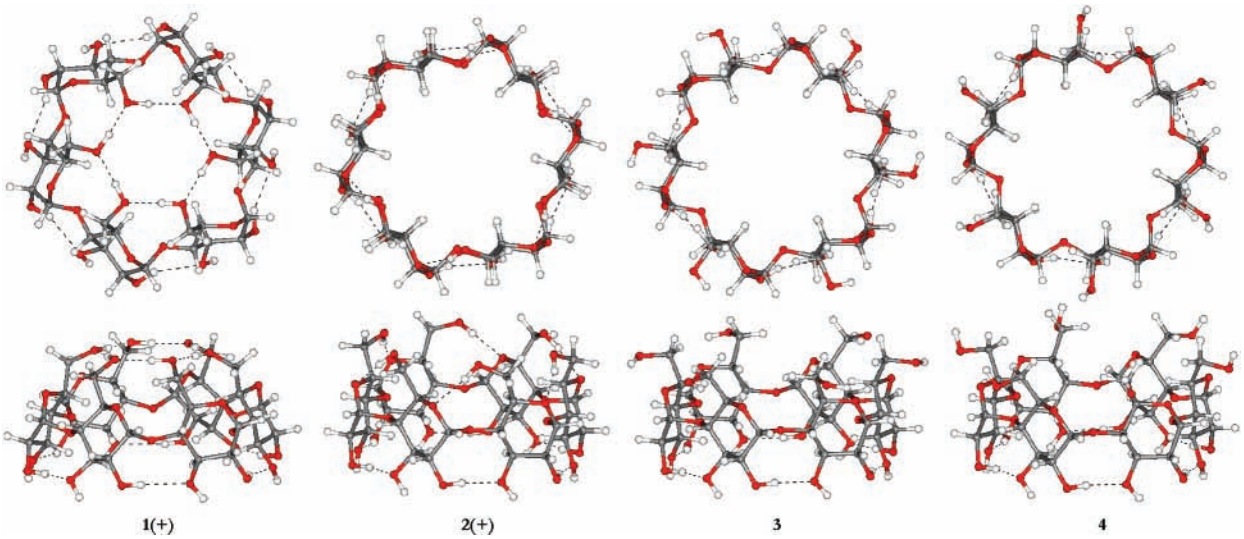

Figure 1. Relevant minimum energy structures located on the BLYP/MBS1 PES for α-CD. In this work, the conformers **1** and **2** exhibit two distinct orientations for secondary hydroxyl groups: right-oriented (+) and left-oriented (−), in accordance with Rudyak et al.[45] The conformers **1(−)** and **2(−)** are not shown in this figure. The structures **3** and **4** have the secondary hydroxyl groups right-oriented (+) and the primary OH groups not making intramolecular hydrogen bonds. For clarity, the notation + for the structures **3** and **4** was omitted, along the text.

effect was taken into account using the polarizable continuum model within the integral equation formalism (IEFPCM)[42,43] in single point calculations, employing BLYP and HF fully optimized gas-phase structures, through the use of the previously defined MBS1 basis set. All calculations in solution were carried out in water ($\epsilon = 78.39$). To improve the quality of the calculated thermodynamic quantities a sequential computational strategy was used for the distinct individual contributions to enthalpy and Gibbs free energy ($T = 298.15$K, $p = 1$ atm). The thermal and solvation energy contributions were evaluated at the BLYP/MBS1 level, and the electronic plus nuclear repulsion energy for a single molecule in a vacuum was calculated using an improved basis set (BLYP/MBS2). The adequacy of this procedure, generally represented by eq 1, has been discussed in refs 22 and 23:

$$\Delta G_{sol} = \Delta E_{elec-nuc}^{BLYP/MBS2} + \Delta G_{T}^{BLYP/MBS1} + \delta\Delta G_{solv}^{BLYP/MBS1} \quad (1)$$

Here ΔG_{sol} is the relative Gibbs free energy in solution (water) calculated at BLYP/MBS2//BLYP/MBS1 and ΔG_T and $\delta\Delta G_{solv}$ are the thermal correction to Gibbs free energy and relative solvation energy, respectively, obtained at the BLYP/MBS1 level.

All calculations were performed at the Laboratório de Química Computacional e Modelagem Molecular (LQC-MM), Departamento de Química, ICEx, UFMG, and Núcleo de Estudos em Química Computacional (NEQC), Departamento de Química, ICE, UFJF, using the Gaussian Program 2003[44] quantum mechanical package.

Results and Discussion

On the basis of the distinct possibilities of hydrogen bond orientations, as mentioned before, some representative free α-CD structures have been submitted for theoretical investigation in the light of the quantum mechanical formalism. In the search for minima on the ab initio PES, various distinct equilibrium structures were found, which do not constitute a complete list. However, six relevant low-energy structures could be selected to be representative conformers of the α-CD. The structures comprise some spatial hydrogen bond arrangement such as alcohol−alcohol or alcohol−ether type in the narrower rim of CD cavity. The conformers studied have been named **1**−**4**, and their optimized geometries are depicted in Figure 1; the notation will be explained.

Structure **1** represents a possible arrangement, reported recently,[25] where the cavity is almost closed in the narrower rim forming a kind of methanol hexamer, while structure **2** exhibit an alcohol−ether type hydrogen bond interaction yielding a close H-bond belt involving both primary and secondary hydroxyls. In the wider rim, the intramolecular H-bonds leads to the formation of rigid belts, named "left-oriented" (−), if the OH group in position 3 acts as the proton donor and the oxygen atom of the OH group in position 2 of the adjacent glucose fragment is the proton acceptor, or "right-oriented" (+), if the OH group in position 2 acts as the proton donor and the oxygen atom of the OH group in position 3 is the acceptor. This is in accordance with the widely used atom numbering for cyclodextrins and the definitions previously reported by Rudyak et al.[45]

It is important to note that structures **1** and **2**, (+) or (−) are relatively rigid due to the complete hydrogen bond belt formed in both sides of CD's cavity leading to a reduced conformational freedom. According to our results, the right-oriented structures **(+)** are more stable than the corresponding left-oriented ones (−), with structure **1(+)** being the gas-phase global minimum. The structures **3** and **4** are also shown in Figure 1. These structures were obtained from modifications on the symmetric structure **2(+)**, where the secondary hydroxyl groups are right-oriented (best orientation). For clarity, the notation + for the structures **3** and **4** was omitted along the text. The primary hydroxyl groups are pointed outside the cavity, in mode parallel (**3**) and perpendicular (**4**). In both structures the primary OH groups do not make intramolecular alcohol−ether type hydrogen bond interactions, therefore being available to interact with solvent and guest molecules.

In Figure 2, the two X-ray structures mentioned previously are also depicted. It is interesting to compare the α-CD X-ray structures (where the hydration waters were omitted) shown in Figure 2 with the relevant minima reported here. It can be clearly seen that our structures **3** and **4** resemble quite well the X-ray II structure, with the primary hydroxyl groups orientation agreeing very well with the X-ray data. The only small

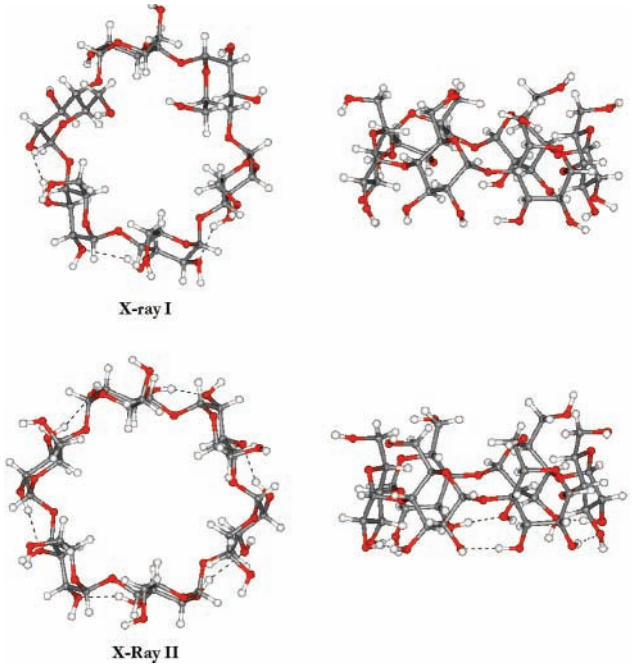

Figure 2. X-ray structures without the water molecules that were excluded for our analysis.

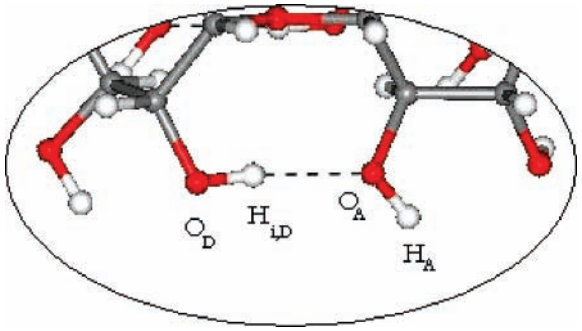

Figure 3. Schematic representation of the partial covalent linked dihedral angle D_i, formed between the identified atoms $H_A-O_A\cdots H_{i,D-}O_D$, where the labels "A" and "D" stand for proton acceptor and proton donor, respectively, and i varies from 1 to 6, according to the number of atoms in α-CD. In addition, we defined the distance R_i as being the distance between $H_{i,D}\cdots O_A$. This dihedral angle definition is for the right-oriented (+) H-bond mode.

difference is the orientation of the secondary hydroxyl groups that in the X-ray geometries were obtained through the aid of a simple calculation, where the positions of the hydrogen atoms were estimated from the difference in Fourier maps,[29,43] therefore, not being truly determined from the X-ray experiment. As will be seen next, this comparison provides a strong indication that the secondary hydroxyl groups are correctly placed in a right-oriented sequence (+), as predicted by our BLYP/MBS1 geometry optimization calculations.

To expand the discussion concerning a comparison of the most similar X-ray structure II to our theoretical results, we carried out a partial geometry optimization keeping the carbon−oxygen backbone frozen (as in the experimental X-ray II structure), employing in the analysis the parameter defined in Figure 3. This was done from the original X-ray structure II. Two partial optimizations have been carried out, both with the frozen X-ray framework, one with orientations of the hydroxyl groups similarly right-oriented as our BLYP/MBS1 structure **3(+)** and another obtained by a partial optimization of the original X-ray structure II (not having a regular (+) or (−) orientation). The data concerning the parameters defined in Figure 3, energy difference and dipole moment, are compiled in Table 1.

TABLE 1: Comparison of Theoretical Data Obtained from BLYP/MBS1 Partial Geometry Optimizations Where the Carbon−Oxygen Skeleton of the X-ray Structure II Was Kept Unchanged and All Primary and Secondary Hydroxyl Groups Were Fully Optimized[a]

param	secondary OH similar to struct **3**	secondary OH similar to struct X-ray II
$\Delta E_{elec-nuc}$ (kcal mol^{-1})	0.0	18.8 (39.0)[c]
μ BLYP/MBS1 (D)	8.637	9.618 (8.894)[d]
H-bond dist (Å)[b]		
R_1	1.907	1.981 (1.939)
R_2	2.174	2.192 (2.156)
R_3	1.853	1.862 (1.907)
R_4	1.750	1.759 (1.713)
R_5	1.966	1.916 (1.950)
R_6	2.006	2.109 (1.999)
dihedral angle (deg)[b]		
D_1	98.6	−15.5[e] (−5.4)
D_2	99.6	101.5 (124.0)
D_3	99.6	106.9 (108.9)
D_4	99.4	−13.2[e] (137.7)
D_5	93.4	−145.3[e] (−119.9)
D_6	100.4	−16.2 (−73.3)

[a] Two orientations for the secondary hydroxyl groups have been used as input in the BLYP geometry optimizations: our global minimum right-oriented **(+)** pattern spatial disposition and the experimental nonregular pattern. The H-bond distance and dihedral angle values in parentheses were obtained from the original nonoptimized X-ray structure II reported in refs 40 and 41. [b] The parameter was defined in Figure 3. [c] BLYP/MBS1 single point energy value for the experimental X-ray II structure from refs 40 and 41. [d] BLYP/MBS1 dipole moment for the experimental X-ray II structure from refs 40 and 41. [e] In this intramolecular H-bond dihedral angle, the secondary hydroxyl is left-oriented (−) with the D and A oxygen atoms being exchanged. So, the new dihedral angle definition is different from the one given in Figure 3: $H_{i,D-}O_D\cdots H_A-O_A$.

It can be seen from Table 1 that there is a good agreement for hydrogen-bond length between the BLYP/MBS1 partially optimized geometrical parameters (keeping the carbon−oxygen skeleton geometry unchanged at the experimental X-ray spatial orientation but optimizing all primary and secondary OH distances, bond angles, and dihedral angles) and the values proposed in the determination of the X-ray structure from the previously cited references. However, the relative BLYP/MBS1 energy values favor considerable our proposed geometry, where the secondary OH groups are all right-oriented (+). The experimentally proposed orientation for these OH groups does not follow a regular right-oriented pattern, as we found to be the best orientation in the gas phase, being rather an irregular mix of oriented and nonoriented H-bond patterns. It was found in this work that the average values for the right- (+) and left-oriented (−) dihedral angles for the secondary hydroxyl groups in structure **2** are respectively 100 and −140 deg. The values reported in the second column of Table 1 agree nicely with the average value for the + structure. However, for the structure optimized using as input the X-ray structure II, only the dihedral angles D_2 and D_3 resemble the expected values for the (+) species. The other four dihedral angles deviate significantly from the average expected values for the (+) and (−) orientations; therefore, the structures optimized on the basis of the X-ray II H-bond pattern lead to nonregular spatial orientations, not having defined (+) and (−) symmetry characteristics. We might be wondering why in the solid state there would be a preference for a totally nonregular H-bond pattern as once based on the

BLYP calculations this is disfavored by almost 20 kcal mol^{-1} (see Table 1).

The central point of this discussion relies on the determination of the best spatial orientation for the hydrogen atoms belonging to the secondary hydroxyl groups that makes intramolecular H-bonds in the solid α-CD and also in water solution. The estimate done in the experimental X-ray made use of a kind of empirical procedure. Our theoretical proposal is based on ab initio calculations for a single molecule, taking into account the electrostatic and van der Waals nature of the intramolecular interactions, which is well-known to be essential for an adequate description of hydrogen bonding. It is quite tempting to believe that our right-oriented mode of interaction should be preferred in the solid state over the irregular hydrogen-bonding pattern proposed in the X-ray determination of the α-CD structure. In the absence of accurate experimental determination of the hydrogen position in the solid-state cyclodextrins, we believe that the approach used here, optimizing only the primary and secondary hydrogen atomic positions keeping the heavy atoms geometry at the X-ray values, provides a satisfactory determination of the hydrogen spatial orientation in cyclodextrins.

Two additional points must be discussed regarding our last statement. First is the adequacy of the theoretical methods to correctly reproduce the hydrogen positions, especially when these atoms are engaged in hydrogen bonding or other kinds of weak interactions. In this case, a high level of theory is needed, including electronic correlation and extended basis sets with inclusion of polarization and diffuse functions. In our methodology such level of theory has been reached for OH groups, supporting the use of the mixed basis set approach to assist the definition of spatial forms of cyclodextrins. The second point is the lack of explicit solvent molecules in the calculations. The X-ray measurements were carried out for hydrated crystals; thus, the flexibility of α-CD allows the molecule to distort in aqueous media. In a previous molecular dynamic study of β-CD in water,[14] using the hybrid QM:MM method, it was showed that the angles Ξ and Ω, defining the spatial arrangements of primary OH, are even more flexible than in the gas phase, following the direction of intermolecular bridges with nearby waters. Hence the intramolecular hydrogen bonds are opened and intermolecular bonds are formed instead. This was also observed for secondary OH,[14] justifying the random orientation of OH groups. Nonetheless the previous arguments do not exclude the forms found in the gas phase, which can play a major role in nonprotic solvents. It is also opportune to mention that in the case of the occurrence of strong hydrogen bonds the correct determination of the proton position is strongly dependent on the level of calculation employed, what becomes a hard computational task.

To describe and compare the structures obtained, we employed in the analysis a considerable number of geometric parameters, most of them reported recently by Brito et al.[46] In addition, we define a new geometric parameter named glucose torsion angle (GTA), basically a parameter that indicates the relative torsion between two glucose units in a sequence, as observed in CDs. The maximum glucose torsion angle (MGTA), in module, is a useful parameter to compare distinct geometries and to infer about the symmetry of CDs. Distorted structures present larger MGTA values. All parameters employed to compare our theoretical fully optimized structures were defined in Figure 4. The parameters used to compare the geometries consist of arithmetic average values between six equivalent distances, bond angles, and dihedral angles in α-CD, taken from each of the four structures. It is noticeable that, except for β,

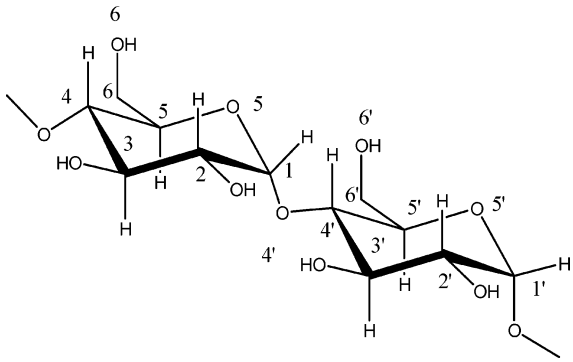

Figure 4. Schematic representation of two glucose units with respective atom numbering, according to the definition of the following geometric parameters employed in this work: Φ, [C2C1O4′C4′]; Ψ, [C1O4′C4′C3′]; Ω, [O5C5C6O6]; Γ, [C1C2C3C4]; T, [C3C4C5O5]; K, [O2C2C1O5]; Y, [O3C3C4C5]; Θ, [C2C3C4C5]; Π, [C4C5O5C1]; Ξ, [C4C5C6O6]; ν, [O4C4C5O5]; Z, [O4C4C5C6]; Λ, [O4′C1O5C5]; E, [O4′C1C4C5]; θ, [C1O4′C4′]; α, [O4O4′O4′′]; β, [O2O3′H2]; GTA (glucose torsion angle), [O5C2C2′O5′].

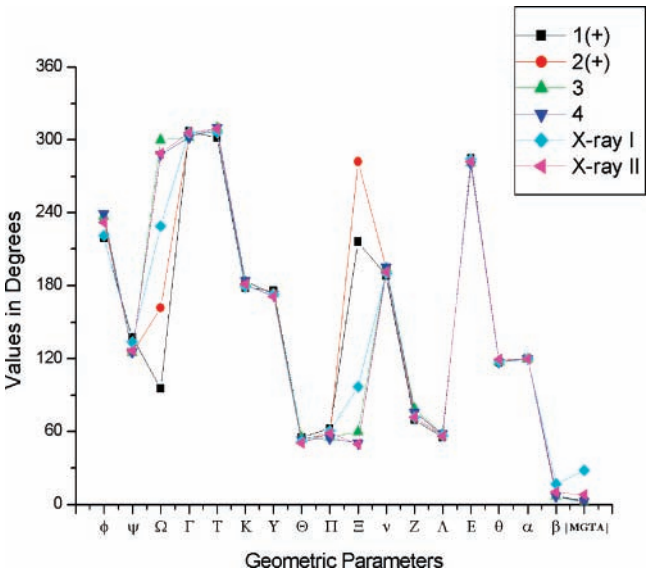

Figure 5. Comparison between all previous defined geometric parameters (Figure 4) for the relevant BLYP/MBS1 fully optimized structures and the two reported X-ray structures. It is noticeable that, except for β, all the other parameters are not sensitive to (+) or (−) secondary hydroxyl group orientations.

all the other parameters are not sensitive to (+) or (−) secondary hydroxyl group orientations.

A comparison of all parameters is given in Figure 5. The backbone of α-CD structure, described by Γ, T, Θ, Π, ν, Z, Λ, E, θ, and α parameters, is kept almost rigid for the four conformers, with the values in good agreement with the solid-state geometry. The Φ and Ψ dihedral angles are related to the relative position of different glucose monomers. For the Φ parameter, an agreement can be observed for structures **1**(+) and X-ray I with the others, including the X-ray II structure, giving larger values by about 15°. In what concerns the Ψ parameter, a similar behavior can be seen for structures **1**(+) and X-ray I, with smaller values by about 10° being found for the others. The dihedrals Ξ and Ω are defined with respect to the primary hydroxyls (O6), which can rotate almost freely for structures **3**, **4**, X-ray I, and X-ray II. Nonetheless, as discussed, the **1** and **2** forms are relatively rigid due to the complete hydrogen bond belt formed on both sides of CD's cavity. Despite the rotational freedom observed for X-ray structures, a considerable number of conformational changes, focused on the primary

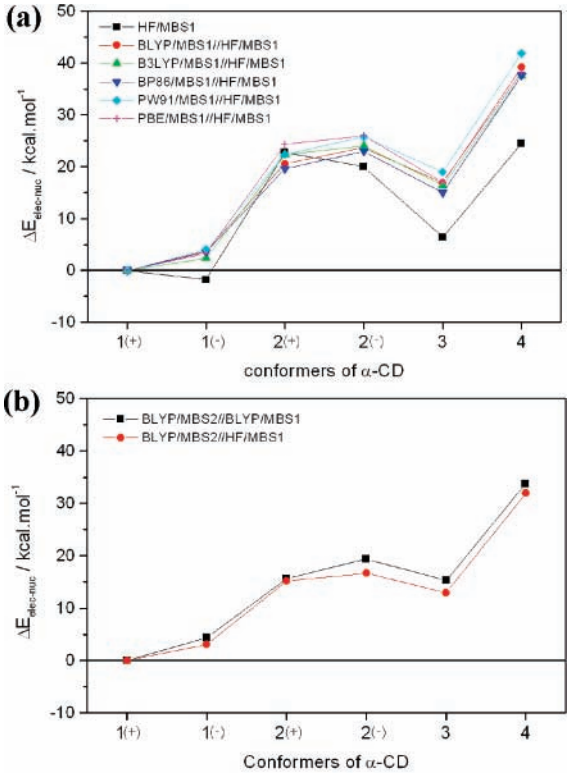

Figure 6. (a) HF/MBS1 and single point DFT/MBS1//HF/MBS1 relative energies for the minimum energy structures located on the PES for the free α-CD species. (b) Comparison between single point BLYP relative energies using BLYP/MBS1 and HF/MBS1 optimized geometries.

hydroxyl groups, are likely to occur, bearing in mind the process X-ray I or II → **1(+)**, in order to increase the Ξ average value. Thus, due to the large value of the Ξ parameter, the conformation **1** is incompatible with any X-ray structure. Similar arguments are valid for structure **2**, in what concerns the parameter Ω.

Different from the flexibility of primary hydroxyls, for all structures studied, the secondary OH groups have quite fixed positions as shown by the constant values of K and Y torsion angles. The average hydrogen-bond angle for secondary hydroxyls (β) is also close to the observed one, although we showed in previous analysis that the predicted relative orientation of O3H and O2H moieties, defined by the dihedral *D* in Figure 3, is quite different from X-ray data (see Table 1). Thus, it can be clearly seen in Figure 5 that the BLYP/MBS1 gas-phase global minimum structure **1(+)** has no significant similarities with any of the two X-ray structures. In addition, structures **3** and **4** show high similarities with the X-ray II, being that the values of the parameters related to structure **4** are very close to the values reported for X-ray II. Considering that X-ray II is stabilized by a ring sequence of six intermolecular hydrogen bonds[41] and its conformation could be predicted as a reasonable intermediate state to the inclusion formation after the exit of the included water molecules and before the entering of the guest molecule, our conformer **4** is the most trustworthy for further studies. However, it does not mean that structure **3** must be rejected, since a conformational interconversion between **3** and **4** would have no energy barrier, once the primary OH groups can rotate freely.

Figure 6a reports HF/MBS1 and single point DFT/MBS1//HF/MBS1 relative energies using as reference the global minimum energy structure in the gas phase, structure **1(+)**, employing various exchange-correlation functionals (BLYP,[32,33,34] B3LYP,[32,33,47] BP86[32,48], PW91,[49,50] PBE[50,51]). It can be seen that the five distinct exchange-correlation functionals used produce the same energy profile, within an uncertainty below ±5 kcal mol^{-1}. Also, the HF relative energies exhibit a considerable deviation compared to the DFT ones, reaching a maximum value of ∼15 kcal mol^{-1}, a quite sizable value, which can be seen as an indication of the importance of electron correlation effects. From the results shown in Figure 6a, it can be concluded that the electron correlation effects, necessary for the description of hydrogen-bond interactions, are consistently reproduced by all functionals used. As it has been reported for some hydrogen-bonded dimers,[52] for molecular complexes where the electrostatic interaction is more relevant than the dispersion contribution to the interaction energy,[53] the BLYP functional performs very satisfactory as compared to high-level ab initio post-HF correlated methods, which validates the use of the BLYP functional to handle the electron correlation effects for the intramolecular hydrogen bonds present in the α-CD species that have definitively an electrostatic nature. Therefore, as long as electrostatic O···H type H-bond interaction is present, there is no need for MP2 or higher correlated level calculation to evaluate relative energies. In this work we will use the BLYP functional to calculate relative energies, as we have done in previous works.[22,23] Figure 6b shows a comparison between BLYP/MBS2//BLYP/MBS1 and BLYP/MBS2//HF/MBS1 relative electronic plus nuclear repulsion energies. From Figure 6b it can be said that, as far as large relative energy values are concerned, the effect of using HF or BLYP fully optimized geometries is not pronounced, with virtually the same energy profile being predicted. The BLYP/MBS2//BLYP/MBS1 and BLYP/MBS2//HF/MBS1 relative energies match very nicely, with a maximum deviation around 2−3 kcal mol^{-1} being observed. This result gives strong support to the use of HF/MBS1 geometries in further theoretical studies involving cyclodextrins. The reason for using the HF level in geometry optimization for large molecular systems is basically the significantly lower computational cost compared to the BLYP level (our experience says that the HF level can be up to five times faster than BLYP to locate a stationary point on the PES for cyclodextrins). In this work, geometry optimizations, harmonic frequency calculations, and the evaluation of PCM relative solvation energies have been done thoroughly at the BLYP level for reason of consistency only. Regarding the PCM solvation energy, in the original work by Barone, Cossi, and Tomasi,[42] all calculations were performed at the HF level employing a standard Pople's split valence basis set[37] and their analysis of the results was also carried out at the HF level. Therefore, it seems natural to calculate geometrical parameters, frequencies, and relative solvation energies at the HF level, which is computational affordable for large molecular systems.

What makes structure **1(+)** the global minimum is the existence of a hydrogen-bonded cluster structure in the smaller cavity side or narrower rim (tail). The alcohol hexamer structure involving the primary hydroxyls present in the gas-phase global minimum structure **1(+)** is shown in Figure 7; first as it appears originally in structure **1(+)** linked to the glucose groups and then as the BLYP/MBS1 fully optimized isolated methanol hexamer structure. The H-bond distance values for the free $(MeOH)_6$ (1.66 Å) are shorter than the corresponding values for the $(MeOH)_6$ present in the cavity of structure **1(+)** (1.77 Å). This can be explained due to the lack of the glucose units in the free hexamer which allow a closer contact of the hydrogen and oxygen atoms. It can be seen that the extra and large stabilization of the α-CD structure **1(+)**, in relation to **2(+)**, is

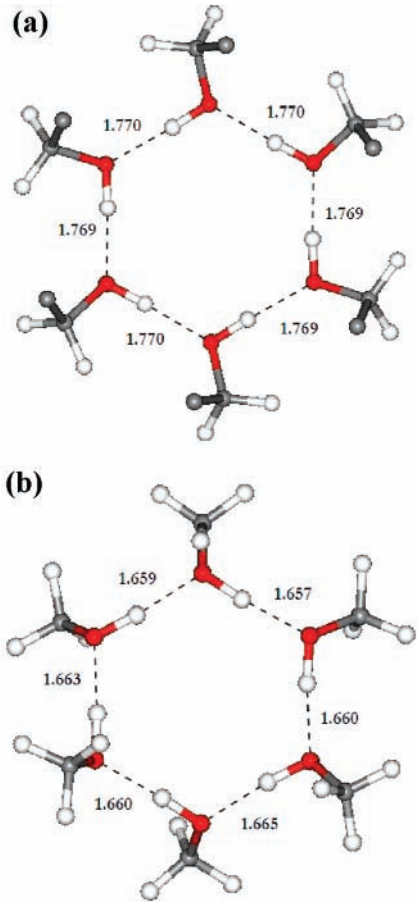

Figure 7. (a) MeOH hexamer original configuration from α-CD structure **1(+)** as found from the BLYP/MBS1 optimized structure (carbon atoms indicated in Figure 7 link the alcohol cluster to the α-CD molecule). (b) $(MeOH)_6$ free structure fully optimized at the BLYP/6-31G(d,p) level.

due to the presence of an alcohol hexamer structure in the cavity side of the primary hydroxyl groups. Our BLYP/6-311++G(2d,2p) relative energy calculations for $(MeOH)_6$ free structure compared to the corresponding methanol−ethyl−ether dimer, which model the structure present in conformer **2(+)**, match nicely the relative preference of structure **1(+)** over structure **2(+)** by 15.6 kcal mol^{-1} reported next in Figure 8. The $(MeOH)_6$ structure is 16.8 kcal mol^{-1} more stable than six times the MeOH−Me_2O ether−alcohol type dimer,[54] which explain the higher preference of structure **1(+)** over **2(+)**. This is always expected in the gas phase, where the formation of larger clusters, encompassing a number of hydrogen-bonding interactions, brings a considerable cooperative effect, therefore, leading to significantly "lower" relative conformational energy values. An interesting point, to be discussed later, is how the situation may be changed in condensed phase, for example in aqueous media.

The individual contributions to the relative Gibbs free energy in solution, i.e., $\Delta E_{ele-nuc}$, ΔG_T, and $\delta\Delta G_{solv}$ (see eq 1), are given in Figure 8. Systematically the thermal correction shifts the equilibrium toward the less symmetric forms **3** and **4**, with the ΔG_T contribution being larger for structure **4**. The solvent effect plays a major role in the equilibrium position, favoring the conformers **2(+)**, **2(−)**, **3**, and **4**. Therefore, in water an equilibrium mixture would be anticipated as confirmed by the relative Gibbs free energy values in solution, which will be shown later in Figure 10.

To complete our investigation of the thermodynamic properties in solution, it may be interesting to analyze the variation

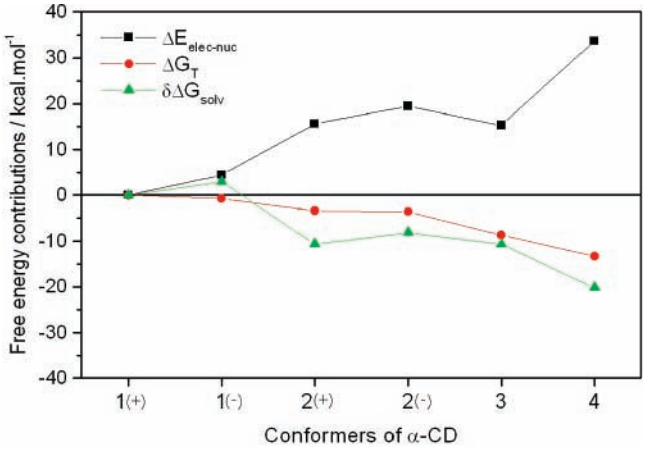

Figure 8. Three individual contributions to the relative Gibbs free energy in solution as given by eq 1. $\Delta E_{elec-nuc}$ was evaluated at the BLYP/MBS2//BLYP/MBS1 level, and the ΔG_T and $\delta\Delta G_{solv}$ quantities were evaluated at the BLYP/MBS1 level of theory.

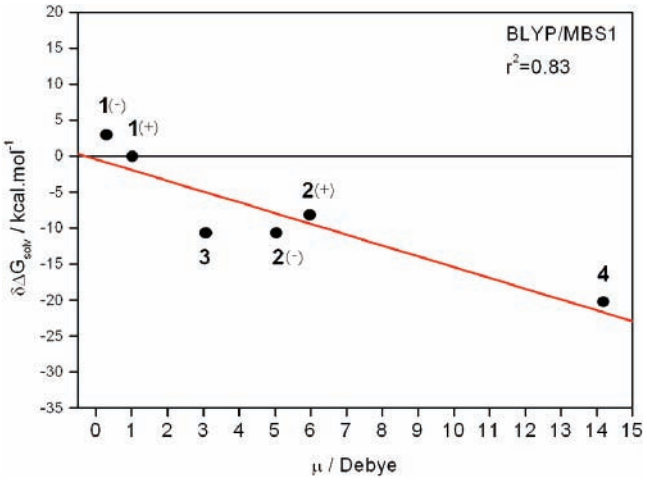

Figure 9. BLYP/MBS1 PCM solvation energies as a function of the gas-phase dipole moment for the relevant minimum energy structure located on the BLYP/MBS1 PES for the free α-CD species.

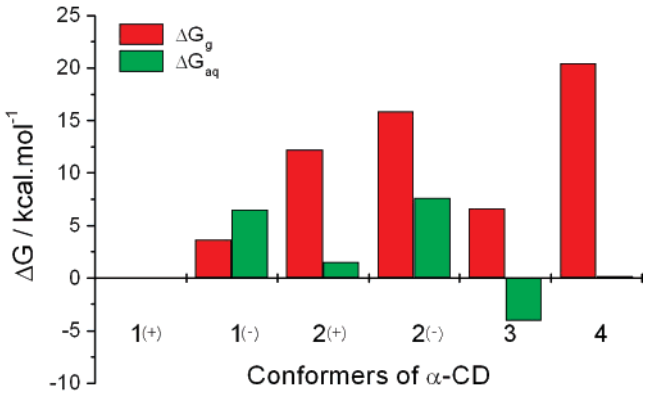

Figure 10. Relative Gibbs free energy (ΔG) values in the gas phase and including solvent effects, calculated using the individual contributions given in Figure 8 at the BLYP/MBS2//BLYP/MBS1 level. $\Delta G_g = \Delta E_{elec-nuc} + \Delta G_T$ and $\Delta G_{aq} = \Delta G_g + \delta\Delta G_{solv}$ as given by eq 1. The conformer **1(+)** was taken as reference.

of the relative solvation energy values ($\delta\Delta G_{solv}$) with the dipole moment (μ) of each conformer, which is shown in Figure 9 for the H_2O solvent at the BLYP/MBS1 level of theory. It can be seen that there is a rough linear dependence between dipole moments and solvation energies, with the more polar form **4** exhibiting the highest solvation energy. Nonetheless other

TABLE 2: Relative Total Energies, Solvation Energies, and Thermodynamic Quantities (in kcal mol^{-1}) Evaluated at the BLYP/MBS2//HF/MBS1 and BLYP/MBS2//BLYP/MBS1 Levels of Calculation

	BLYP/MBS2//HF/MBS1						BLYP/MBS2//BLYP/MBS1					
param	**1(+)**	**1(−)**	**2(+)**	**2(−)**	**3**	**4**	**1(+)**	**1(−)**	**2(+)**	**2(−)**	**3**	**4**
$\Delta E_{elec-nuc}$	0.0	3.1	15.2	16.7	12.9	32.0	0.0	4. 4	15.6	19.4	15.3	33.7
ΔG_T	0.0	−0.3	−2.6	−2.8	−6.6	−10.6	0.0	−0.8	−3.4	-3.6	−8.7	−13.3
$\delta\Delta G_{solv}$	0.0	2.3	−13.0	−11.3	−15.8	−24.9	0.0	2. 9	−10.7	-8.2	−10.7	−20.2
ΔG_g	0.0	2.8	12.6	13.9	6.3	21.4	0.0	3. 6	12.2	15.8	6.6	20.4
ΔG_{aq}	0.0	5.1	−0.4	2.6	−9.5	−3.5	0.0	6. 5	1.5	7.6	−4.1	0.2

structural and electronic distribution aspects of each minimum energy structure may also play an important role, according to the PCM continuum solvation model.[42] It was observed (data not shown) that the water solvent produces larger relative solvation energy than $CHCl_3$ ($\epsilon = 4.9$), except for structure **1(−)**, which can be easily rationalized in terms of the lowest dipole moment value, as can be seen from Figure 9. Therefore, we expect that the PCM model may be satisfactory for the investigation of the plausible structures of α-CD that can coexist in equilibrium in water solution. It is opportune to say that the ability of the PCM model to reproduce accurately absolute solvation energies in water may be questioned, owing to the presence of empirical parameters and definition of the cavities, and also it may exhibit a lack of physical significance in the evaluation of free energy of solvation terms. However, when relative energy values are calculated, as presented here for α-CD species, a significant error cancellation is expected to take place and so relative solvation energies can be considered as satisfactorily reliable to be used in the area of supramolecular chemistry.

Finally, in Figure 10 the relative Gibbs free energy, including all contributions, is shown, taking the form **1(+)** as reference for calculation. Considering only the enthalpy values (data not shown), the structure **1(+)** is still preferred in aqueous media by at least 5 kcal/mol; however, when entropic effects are accounted for combined with the PCM solvation model, structure **3** is the preferred one in water solution. Due to the small free energy difference in solution, it can be said that there will probably be a conformation mixture at room temperature containing as strong candidates in water solution structures **1(+)**, **2(+)**, **3**, and **4**, with a significantly larger proportion of structures **3**. The main results from this work are compiled in Table 2, calculated at the BLYP/MBS2//HF/MBS1 and BLYP/MBS2//BLYP/MBS1 levels (where the double slash means that a BLYP/MBS2 single point energy calculation was performed at either HF/MBS1 or BLYP/MBS1 fully optimized geometry). Using as reference the BLYP/MBS2//HF/MBS1 level of calculation, the predicted relative stability of the relevant six minimum energy structures located on the HF/MBS1 PES of α-CD in the gas phase is (with relative energies in kcal mol^{-1} given in parentheses) the following: **1(+)** (0.0); **1(−)** (3.1); **3** (12.9); **2(+)** (15.2); **2(−)** (16.7); **4** (32.0). This same trend is found when BLYP/MBS1 geometry is considered. It can be seen from Table 2 that structure **3** is preferred in water solution at both levels with the solvent playing a primary role. As shown in Figure 6b, the use of the HF/MBS1 geometry accounts for a deviation of 2−3 kcal mol^{-1} in the relative energy values; however. the solvation energy contribution provides a larger stabilization of the other structures in relation to the gas-phase global minimum structure **1(+)**.

Conclusion

The PES for the α-CD species was extensively investigated at the ab initio HF and BLYP levels of calculation, using a mixed basis set, 6-31G(d,p)/STO-3G (named MBS1). Six true minimum energy structures were located on the BLYP/MBS1 PES, characterized through harmonic frequency calculations. Thermal correction and solvation energy (using the PCM model and water as solvent) contributions were evaluated at the HF/MBS1 and BLYP/MBS1 levels of theory. Therefore, relative enthalpy and Gibbs free energy values in the gas phase and water solution could be calculated. We found that structure **1(+)**, having an alcohol hexamer structure at the smaller rim, is the preferred one in the gas phase at room temperature, while structure **3**, which resembles the crystallographic structure II, is expected to be predominant in aqueous media.

By comparing relative energies from HF and DFT levels, we conclude that while the HF method is satisfactory for structural determination, ab initio methods including electron correlation effects must be used to calculate relative energies for cyclodextrin and also other supramolecular systems where intramolecular hydrogen bonds are present. Therefore, the BLYP/MBS2//HF/MBS1 approach may be a valuable procedure, computationally affordable, for investigating the structure and thermodynamic properties in the gas phase and water solution of supramolecular systems.

From the analysis of the structural parameters, we observed that the number of hydrogen bonds formally formed contributes in a majority way to the stabilization of the conformations showed here. The electronic plus nuclear repulsion energy is directly affected by the formation of this kind of interaction. Nevertheless this contribution loses main status in the condensed phase due to the increasing importance of symmetry, represented by the dipole values, and the intermolecular interactions which could exist in solution.

Probably in aqueous solution the structural arrangement of α-CD would be similar to the crystallographic geometry X-ray II, through its relative stability at condensed phase calculations. To guide future theoretical works about cyclodextrins and their inclusion complexes in aqueous solution, we could say that care is needed to handle the theoretical results. The stabilization and predicted existence of these structures can be drastically changed with the inclusion of solvent effect and, therefore, modify the conclusions and the understanding of the thermodynamics of the inclusion formation process.

Acknowledgment. We thank the Brazilian agencies CNPq (Conselho Nacional de Desenvolvimento Científico e Tecnológico) and FAPEMIG (Fundação de Amparo à Pesquisa do Estado de Minas Gerais) for financial support. This work is part of the project PRONEX-FAPEMIG/EDT-537/05.

References and Notes

(1) Connors, K. A. *Chem. Rev.* **1997**, *97*, 1325−1357.
(2) Dodziuk, H. *Introduction to supramolecular chemistry*; Kluwer Publishers: Amsterdam, 2002.
(3) Barr, L.; Dumanski, P. G.; Easton, C. J.; Harper, J. B.; Lee, K.; Lincoln, S. F.; Meyer, A. G.; Simpson, J. S. *J. Inclusion Phenom. Macrocyclic Chem.* **2004**, *50*, 19−24.
(4) Harada, A. *Acc. Chem. Res.* **2001**, *34* (6), 456−464.

(5) Wenz, G.; Han, B. H.; Muller, A. *Chem. Rev.* **2006**, *106*, 782−817.
(6) Easton, C. J.; Lincoln, S. F. *Modified Cyclodextrins: Scaffold and Templates for Supramolecular Chemistry*; Imperial College Press: London, 1999.
(7) Harada, A. *Supramol. Sci.* **1996**, *3*, 19−23.
(8) Dodziuk, H.; Kozminski, W.; Ejchart, A. *Chirality* **2004**, *16*, 90−105.
(9) Bea, I.; Jaime, C.; Kollman, P. *Theor. Chem. Acc.* **2002**, *108*, 286−292.
(10) (a) Blenke, C.; Da Silva, V. J.; Junqueira, G. M. A.; De Almeida, W. B.; Dos Santos, H. F. *J. Mol. Struct. (Theochem*) **2007**, *809*, 95−102. (b) Castro, E. A.; Nascimento, C. S., Jr.; Barbiric, D. A. J.; De Almeida, W. B.; Dos Santos, H. F. *Mol. Simul.* **2006**, *32*, 623.
(11) Rekharsky, M. V.; Inoue, Y. *Chem. Rev.* **1998**, *98*, 1875−1917.
(12) Dodziuk, H. *J. Mol. Struct.* **2002**, *614*, 33−45.
(13) Lipkowitz, K. B. *Chem. Rev.* **1998**, *98*, 1829−1873.
(14) Heine, T.; Dos Santos, H. F.; Patchkovskii, S.; Duarte, H. A. *J. Phys. Chem. A* **2007**, *111*, 5648−5654.
(15) Dodziuk, H.; Lukin, O.; Nowinski, K. S. *J. Mol. Struct. (Theochem)* **2000**, *503*, 221−230.
(16) Bea, I.; Gotsev, M. G.; Ivanov, P. M.; Jaime, C.; Kollman, P. A. *J. Org. Chem.* **2006**, *71*, 2056−2063.
(17) Bonnet, P.; Jaime, C.; Morin-Allory, L. *J. Org. Chem.* **2002**, *67*, 8602−8609.
(18) Castro, E. A.; Barbiric, D. A. J. *J. Argent. Chem. Soc.* **2002**, *90*, 1.
(19) Castro, E. A.; Barbiric, D. A. J. *Curr. Org. Chem.* **2006**, *10*, 715−729.
(20) Jaime, C.; de Federico, M. *Curr. Org. Chem.* **2006**, *10*, 731−743.
(21) Dodziuk, H.; Lukin, O. *Chem. Phys. Lett.* **2000**, *327*, 18−22.
(22) Nascimento, C. S.; Anconi, C. P. A.; Dos Santos, H. F.; De Almeida, W. B. *J. Phys. Chem. A* **2005**, *109*, 3209−3219.
(23) Nascimento, C. S.; Dos Santos, H. F.; De Almeida, W. B. *Chem. Phys. Letters* **2004**, *397*, 422−428.
(24) Nascimento, C. S.; Anconi, C. P. A.; Dos Santos, H. F.; De Almeida, W. B. *J. Inclusion Phenom. Macrocyclic Chem.* **2007**, 10.1007/s10847−007-9320-5.
(25) (a) Pinjari, R. V.; Joshi, K. A.; Gejji, S. P. *J. Phys. Chem. A* **2006**, *110*, 13073−13080. (b) Karpfen, A.; Liedl, E.; Snor, W.; Weiss-Greiler, P.; Viernstein, H.; Wolschann, P. *J. Inclusion Phenom. Macrocyclic Chem.* **2007**, *57*, 35−38.
(26) Manor, P. C.; Saenger, W. *Nature* **1972**, *237*, 392.
(27) Manor, P. C.; Saenger, W. *J. Am. Chem. Soc.* **1974**, *96*, 3630−3639.
(28) McMullan, R. K.; Saenger, W.; Fayos, J.; Mootz, D. *Carbohydr. Res.* **1973**, *31*, 37−46.
(29) Chacko, K. K.; Saenger, W. *J. Am. Chem. Soc.* **1981**, *103*, 1708−1715.
(30) Szejtli, J. *Chem. Rev.* **1998**, *98*, 1743−1753.
(31) Dos Santos, H. F.; Duarte, H. A.; Sinisterra, R. D.; Mattos, S. V. D.; De Oliveira, L. F. C.; De Almeida, W. B. *Chem. Phys. Lett.* **2000**, *319*, 569−575.
(32) Becke, A. D. *Phys. Rev. A* **1988**, *38*, 3098−3100.
(33) Lee, C.; Yang, W.; Parr, R. G. *Phys. Rev. B* **1988**, *37*, 785.
(34) Miehlich, B.; Savin, A.; Stoll, H.; Preuss, H. *Chem. Phys. Lett.* **1989**, *157*, 200−206.
(35) Hehre, W. J.; Stewart, R. F.; Pople, J. A. *J. Chem. Phys.* **1969**, *51*, 2657−2664.
(36) Collins, J. B.; Schleyer, P. v. R.; Binkley, J. S.; Pople, J. A. *J. Chem. Phys.* **1976**, *64*, 5142−5151.
(37) (a) Ditchfield, R.; Hehre, W. J.; Pople, J. A. *J. Chem. Phys.* **1971**, *54*, 724. (b) Hehre, W. J.; Ditchfield, R.; Pople, J. A. *J. Chem. Phys.* **1972**, *56*, 2257. (c) Hariharan, P. C.; Pople, J. A. *Mol. Phys.* **1974**, *27*, 209. Gordon, M. S. *Chem. Phys. Lett.* **1980**, *76*, 163. (e) Hariharan, P. C.; Pople, J. A. *Theor. Chim. Acta* **1973**, *28*, 213. (f) Binning, R. C., Jr.; Curtiss, L. A. *J. Comput. Chem.* **1990**, *11*, 1206.
(38) (a) Krishnan, R.; Binkley, J. S.; Seeger, R.; Pople, J. A. *J. Chem. Phys.* **1980**, *72*, 650. (b) McLean, A. D.; Chandler, G. S. *J. Chem. Phys.* **1980**, *72*, 5639. (c) Clark, T.; Chandrasekhar, J.; Spitznagel, G. W.; Schleyer, P. v. R. *J. Comput. Chem.* **1983**, *4*, 294. (d) Frisch, M. J.; Pople, J. A.; Binkley, J. S. *J. Chem. Phys.* **1984**, *80*, 3265.
(39) See for example: McQuarrie, D. A. *Statistical Thermodynamics*; University Science Books: Mill Valley, CA, 1973.
(40) CSD: http://www.ccdc.cam.ac.uk/, C. S. D., In.
(41) Puliti, R.; Mattia, C. A.; Paduano, L. *Carbohydr. Res.* **1998**, *310*, 1−8.
(42) Barone, V.; Cossi, M.; Tomasi, J. *J. Chem. Phys.* **1997**, *107*, 3210−3221.
(43) Cossi, M.; Barone, V.; Cammi, R.; Tomasi, J. *Chem. Phys. Lett.* **1996**, *255*, 327−335.
(44) Frisch, M. J.; et al. *Gaussian 2003*, revision B.04; Gaussian: Pittsburgh, PA, 2003.
(45) Rudyak, V. Y.; Avakyan, V. G.; Nazarov, V. B.; Voronezheva, N. I. *Russ. Chem. Bull.* **2006**, *55*, 1337−1345.
(46) Britto, M.; Nascimento, C. S.; dos Santos, H. F. *Quim. Nova* **2004**, *27*, 882−888.
(47) Becke, A. D. *J. Chem. Phys.* **1993**, *98*, 5648−5652.
(48) Perdew, J. P. *Phys. Rev. B* **1986**, *33*, 8822.
(49) Burke, K. P.; J. P.; Wang, Y. *Eletronic Density FUnctional Theory: Recent Progress and New Directions*; Springer: New York, 1988.
(50) Perdew, J. P.; Burke, K.; Wang, Y. *Phys. Rev. B* **1996**, *54*, 16533−16539.
(51) Perdew, J. P.; Burke, K.; Ernzerhof, M. *Phys. Rev. Lett.* **1997**, *78*, 1396−1396.
(52) De Almeida, W. B. *J. Braz. Chem. Soc.* **2005**, *16*, 345−361.
(53) Chalasinski, G.; Szczesniak, M. M. *Chem. Rev.* **1994**, *94*, 1723−1765.
(54) De Almeida, W. B. Private communication. In Belo Horizonte.